European Journal of Pharmaceutics and Biopharmaceutics 83 (2013) 131–140

Contents lists available at SciVerse ScienceDirect

European Journal of Pharmaceutics and Biopharmaceutics

journal homepage: www.elsevier.com/locate/ejpb

Research paper

Low molecular weight oligochitosans for non-viral retinal gene therapy

G. Puras [a,b], J. Zarate [a,b], M. Aceves [a,b], A. Murua [a,b], A.R. Díaz [b,c], M. Avilés-Triguero [d], E. Fernández [b,c], J.L. Pedraz [a,b,*]

[a] NanoBioCel Group, University of Basque Country, Vitoria, Spain
[b] Networking Research Centre of Bioengineering, Biomaterials and Nanomedicine (CIBER–BBN), Spain
[c] Neuroprothesis and Neuroengineering Research Group, Miguel Hernández University, Spain
[d] Laboratory of Experimental Ophthalmology, Faculty of Medicine, University of Murcia, Regional Campus of International Excellence "Campus Mare Nostrum", Murcia, Spain

ARTICLE INFO

Article history:
Received 26 July 2012
Accepted in revised form 8 September 2012
Available online 8 October 2012

Keywords:
Gene therapy
Chitin/chitosan
Molecular weight
Nanoparticles
Retina

ABSTRACT

Ultrapure oligochitosans have recently been evaluated as a promising tool for corneal gene therapy; however, there are no reports regarding the potential use of this polymer in other ocular tissues. We have prepared and characterized at pH 7.1 oligochitosan/pCMS-EGFP polyplexes to evaluate the transfection efficiency in rat retinas after subretinal and intravitreal administration. Polyplexes were characterized in terms of shape, size, surface charge, DNA condensation, and transfection efficiency in HEK-293 and ARPE-19 culture cells. Polyplexes were positively charged, around 10 mV, and size oscillated between 256.5 ± 56 and 67.3 ± 0.44 nm, depending on the nitrogenous/phosphate ratio. Polyplexes efficiently protected the plasmid against enzymatic digestion. A drastic increase in transfection efficiency was observed when pH slightly decreased from 7.4 to 7.1 in both HEK-293 (from 19.1% to 51.5%) and ARPE-19 (from 2.0% to 36.5%) cells (data normalized to Lipofectamine™ 2000). In rat retinas, subretinal administrations transfected cells mainly in the RPE layer, whereas intravitreal injections transfected cells in the inner nuclear and plexiform layers of the retina and mainly in the ganglion cell layer. This study establishes the base for future treatments of genetic retinal disorders with low molecular weight oligochitosan polyplexes.

© 2012 Elsevier B.V. All rights reserved.

1. Introduction

Gene therapy represents an attractive approach to treat many inborn or acquired diseases by producing bioactive agents, replacing defective genes or silencing unwanted gene expression. The therapeutic application of genes demands appropriate safe carriers to mammalian cells, since naked therapeutic genes need to be protected mainly from Deoxyribonuclease (DNase) degradation to avoid low transfection efficiency [1]. Therefore, one of the essential prerequisites for successful gene therapy relies on the development of safe and effective carriers [1,2]. At present, the vectors used today can be classified in two main groups: viral and non-viral vectors. Viral-based carriers are the most effective; however, their application to human body is limited by potential infectivity, inflammation, immunogenicity, and the small size of the DNA they can transport [3–5]. On the other hand, non-viral vector-based formulations are being extensively studied mainly due to some important advantages such as the absence of DNA size limit, non-infectivity, less immunogenicity, low cost, and easy production [6]. Among non-viral vectors, chitosan-based formulations have gained increasing attention as safe gene carrier candidates [7–10]; however, the low transfection efficiency of chitosans represents an important handicap for clinical applications. Many studies conducted on chitosan/DNA systems indicate that transfection efficiency depends on several factors such as the degree of deacetylation (DDA) and molecular weight (MW) of the chitosan, the pH and the serum concentration of the transfection medium, the charge ratio of chitosan to DNA (*N*/*P* ratio) and the cell type [11–17]. In this study, we designed polyplexes based on NOVAFECT O15, an ultrapure oligochitosan that easily form polyplexes with DNA through electrostatic interactions [18] and characterized their physicochemical properties in terms of shape, size, surface charge and DNA condensation, protection, and release capacity. The most biotechnologically suitable formulations were selected for *in vitro* transfection studies at pH 7.4 (following the standard conditions of the manufacturer's protocol) and at pH 7.1, because has been widely reported that chitosan-mediated transfection strongly depends on slight changes in the pH value of the transfection medium [11,15]. Transfection efficiency of polyplexes was evaluated in Human Embryonic Kidney (HEK-293) culture cells, one of the most employed models for transfection studies, and in a more

* Corresponding author. Laboratory of Pharmacy and Pharmaceutical Technology, Faculty of Pharmacy, University of the Basque Country, 01006 Vitoria-Gasteiz, Spain. Tel.: +34 945013091; fax: +34 945013040.
E-mail address: joseluis.pedraz@ehu.es (J.L. Pedraz).

0939-6411/$ - see front matter © 2012 Elsevier B.V. All rights reserved.
http://dx.doi.org/10.1016/j.ejpb.2012.09.010

Table 1
Oligochitosan/DNA polyplexes formulations with a DNA concentration of 13.2 μg/ml at different *N*/*P* ratios.[a]

	N/*P* charge ratio					
	10:1 (μl)	20:1 (μl)	30:1 (μl)	40:1 (μl)	50:1 (μl)	60:1 (μl)
Plasmid (0.5 mg/ml)	13.2	13.2	13.2	13.2	13.2	13.2
NOVAFECT (2 mg/ml)	22.1	44.2	66.5	88.4	110.5	133
Ultrapure water	464.7	442.6	420.3	398.4	376.3	353.8
Total volume (μl)	500	500	500	500	500	500

[a] If a concentration of plasmid DNA higher than 13.2 μg/ml is required, manufacturer's protocol recommends mixing the reagent and the plasmid DNA at approximately 1:1 (v/v) ratio to avoid aggregation.

difficult cell line to be transfected, as the Human Retinal Pigmented Epithelial Cells (ARPE-19).

Because of the mucoadhesive and the low cytotoxicity properties of the oligochitosans, polyplexes based on these formulations have been successfully used for *in vivo* delivery of genes to mucosal tissues [19,20]. Regarding the ocular system, a privileged organ for local gene therapy [21], non-viral carriers such as peptides [22], liposomes [23,24], solid lipid nanoparticles [24], and polymers [25] gained increasing attention since the 1990s. Among polymers, chitosan-based formulations have been extensively studied for ocular therapy purposes [26,27]; however, ultrapure oligochitosans as NOVAFECT O15 have been only studied for corneal gene delivery after intraestromal injection [18,28]. Therefore, in order to elucidate the potential application of ultrapure oligochitosans as DNA carriers in other ocular tissues such as the retina, we administered these polyplexes by subretinal and intravitreal injections to the posterior segment of the rat eye, where the pH 7.1 is slightly more acidic than either plasma or aqueous humor [29], and evaluated the expression of the EGFP after 72 h in different cells and layers of the retina by confocal microscopy.

2. Materials and methods

2.1. Materials

NOVAFECT O15 with a molecular weight of 5.7 kDa, a DDA ⩾97%, acetate salt and endotoxin levels ⩽0.05 EU/mg, was purchased from NovaMatrix/FMC (Sandvika, Norway). HEK-293 and ARPE-19 were obtained from the American Type Culture Collection (ATCC). The plasmid pCMS-EGFP, which encodes the enhanced green fluorescent protein (EGFP), was purchased from BD Biosciences Clontech (Palo Alto, California, USA) and amplified by Dro Biosystems S.L. (San Sebastian, Spain). The gel electrophoresis materials and ethidium bromide solution were acquired from Bio-Rad (Madrid, Spain). DNase I, lauryl sulfate sodium (SDS), phosphate buffer solution (PBS), HEPES MES, and sodium bicarbonate reagent were purchased from Sigma–Aldrich (Madrid, Spain). Cell culture reagents were purchased from LGC Promochem (Barcelona, Spain), Opti-MEM® I reduced medium, antibiotic/antimicotic solution, and Lipofectamine™ 2000 transfection reagents were acquired from Invitrogen (San Diego, California, USA). The BD-via Probe kit was provided by BD Biosciences (Belgium). Adult Sprague–Dawley rats were purchased from Harlan Laboratories (Barcelona, Spain).

2.2. Preparation of oligochitosan/DNA polyplexes

Oligochitosan/DNA polyplexes having a DNA concentration of 13.2 μg/ml with different *N*/*P* ratios were prepared by the self-assembly method according with the instructions of the manufacturer and adapted to a final volume of 500 μl. Briefly, the DNA stock solution was diluted in ultrapure water, and the oligochitosan stock solution was added to the plasmid DNA water mixture under vortex mixing (1200 rpm) for at least 10 s and subsequently equilibrated at room temperature for 30 min before performing transfection experiments. An example of a series of formulations of oligochitosan/DNA polyplexes is shown in Table 1.

2.3. Cryo-Transmission Electron Microscopy (Cryo-TEM)

Oligochitosan/DNA polyplexes at a fixed *N*/*P* ratio of 20 were observed by Cryo-TEM microscopy. Briefly, one drop of the sample solution was vitrified by rapid freezing in liquid ethane using a Vitrobot Markt IV (FEI). This vitrified sample grid was transferred through 655 Turbo Pumping Station (Gatan) to a 626 DH Single Tilt Liquid Nitrogen Cryo-holder (Gatan), where was maintained about −180 °C. Copper grid (300 mesh Quantifoils) was hydrophilized by glow-discharge treatment. The sample was examined in a TEM, TECNAI G2 20 TWIN (FEI), operating at an accelerating voltage of 200 keV in a bright-field and low-dose image mode.

2.4. Measurements of size and zeta potential

The hydrodynamic diameter of the polyplexes was determined by dynamic light scattering (DLS) based on backscatter detection optics at 173°. Briefly, polyplexes (100 μl) were resuspended into HEPES medium (1400 μl, 10 mM, pH 7.1), and size was determined using Zetasizer NanoZS (Malvern Instruments, UK). All measurements were carried out in triplicate. The particle size reported as hydrodynamic diameter was obtained by cumulative analysis.

Zeta potential measurements were obtained by laser doppler velocimetry (LDV) after resuspending the polyplexes (100 μl) into the same HEPES medium (1400 μl, 10 mM, pH 7.1) in disposable folded capillary cells for zeta analysis. The Smoluchowski approximation was used to support the calculation of the zeta potential from the electrophoretic mobility. Zeta potential measurements were run in triplicate. Only data that met the quality criteria according with the software program (DTS 5.0, Zetasizer Nanosystem) were included in the study.

2.5. Agarose gel electrophoresis assay

The capacity of the oligochitosans to complex, release, and protect DNA from DNase I enzymatic digestion was estimated by a gel retardation assay based on agarose gel electrophoresis. Naked DNA or samples of polyplexes at different *N*/*P* ratio (20 μl, containing 200 ng of the plasmid) were loaded to an agarose gel (0.8%) that contained 1% of ethidium bromide for visualization. The gel was immersed in a Tris–acetate–EDTA buffer and exposed for 30 min to 120 V. Bands were observed with a model TFX-20 M transilluminator (Vilber-Lourmat), and the images were captured using a DigiDoc digital camera from BioRad. To estimate the capacity of oligochitosans to release DNA from polyplexes, 20 μl of a 2% SDS solution was added to the samples resulting in a final concentration of 1%. Protection capacity against enzymatic digestion was studied after adding DNase I (final concentration of 1 U DNase I/

2.5 μg DNA) to polyplexes. The mixtures were incubated at 37 °C for 30 min. Afterward, 2% SDS solution was added to release DNA from polyplexes. The integrity of the DNA in each sample was compared with untreated DNA.

2.6. Cell culture and transfection protocols

"*In vitro*" assays were performed with two different cell lines: HEK-293 and ARPE-19. HEK-293 cells were maintained as monolayer culture in Eagle's Minimal Essential medium (EMEM) with Earle's BSS and 2 mM L-glutamine supplemented with 10% heat-inactivated horse serum and 1% antibiotic/antimycotic. Cells were incubated at 37° C under 5% CO_2 atmosphere and subcultured every 2–3 days. ARPE-19 cells were maintained in Dulbecco's Modified Eagle's Medium–Han's Nutrient Mixture F-12 (1:1) medium (D-MEM/F-12) supplemented with 10% heat-inactivated fetal calf serum and 1% antibiotic/antimycotic solution. Cells were incubated at 37° C under 5% CO_2 atmosphere and subcultured every 4–5 days. For transfection studies, HEK-293 and ARPE-19 cells were seeded without any antibiotic on 24 well plates at a density of 150,000 and 100,000 cells per well, respectively, and allowed to adhere overnight to reach 70–90% of confluence at the time of transfection. Then, the regular growth media was removed and the cells were exposed to polyplexes containing 1.65 μg of the EGFP pDNA and adequate amounts of oligochitosans (see Table 1). Formulations for transfection were prepared after mixing 1:1 polyplexes and hypertonic (580 mM) serum-free transfection medium (Opti-MEM® I, pH 7.4 containing 270 mM mannitol), so that the final formulation is isotonic. Cells were then carefully washed with PBS, and 250 μl of the transfection formula was added to each well. Each formulation was used in triplicate for statistical analysis. After 4 h of incubation at 37 °C, the transfection medium was replaced by 500 μl of regular growth medium, pH 7.4. Cells were allowed to grow for 72 h until fluorescent microscopy and flow cytometry analyses. Transfection experiments at pH 7.1 were performed as previously described, but adding 10 mM HEPES to the hypertonic serum-free Opti-MEM® I transfection medium. The pH value of the transfection medium was adjusted with 1 N HCl the same day of the transfection and filtered with Millipore 0.22 μm PVC filters (Madrid, Spain). After 4 h of incubation at 37 °C, the transfection medium (pH 7.1) was replaced by 500 μl of regular growth medium, pH 7.4, and cells were allowed to grow until fluorescent microscopy and flow cytometry analyses (72 h). Experiments with Lipofectamine™ 2000/pDNA complexes were prepared at a 2/1 ratio (μg) according to the manufacturer's protocol.

2.7. Transfection efficiency and cell viability measurement

Qualitative expression of EGFP was examined 72 h post-transfection using an inverted microscope with simultaneous epi-fluorescence and phase contrast observation (Eclipse TE200-S, Nikon Instruments Europe B.V., Amstelveen, The Netherlands). Images were captured with a 20× objective. Flow cytometry analysis was conducted on a FACSCalibur system flow cytometer (Becton Dickinson Biosciences, San Jose, USA). Briefly, cells were washed twice with PBS and detached with 300 μl of 0.05% trypsin/EDTA. Then, cells were centrifuged and the supernatant was discarded. The pellet was resuspended in PBS, diluted in FACSFlow liquid, and directly introduced in the flow cytometer. Transfection efficiency was expressed as the percentage of EGFP positive live cells at 525 nm (FL_1). For cell viability measurements, the BD-via Probe reagent (5 μL) was added to each sample to exclude dead cells from the analysis. The fluorescence corresponding to dead cells was measured at 650 nm (FL_3). Control samples (non-transfected cells) were displayed on a forward scatter (FSC) versus side scatter (SSC) dot-plot to establish a collection gate and exclude cells debris. Other samples containing Lipofectamine transfected cells without BD-via Probe and non-transfected cells with BD-via Probe were used as controls to compensate the FL_2 signal in FL_1 and FL_3 channels. For each sample, 10,000 events were collected.

2.8. Animals and anesthetics

Adult male Sprague–Dawley rats (6–7 weeks old and 150–200 g body weight) were used as experimental animals in this study. Rats were housed in temperature and light controlled rooms with a 12 h light/dark cycle and had food and water *ad libitum*. All experimental procedures were carried out in accordance with the Spanish and European Union regulations for the use of animals in research and the Association for Research in Vision and Ophthalmology (ARVO) statement for the use of animals in ophthalmic and vision research and supervised by the Miguel Hernandez University Standing Committee for Animal Use in Laboratory. Adequate measures were taken to minimize pain or discomfort. All the experimental manipulations were carried under general anesthesia induced with an intraperitoneal (i.p.) injection of a mixture of ketamine (70 mg/kg, Ketolar®, Parke–Davies, S.L., Barcelona, Spain) and xylazine (10 mg/kg, Rompún®, Bayer, S.A., Barcelona, Spain). For recovery from anesthesia, rats were placed in their cages and an ointment containing tobramycin (Tobrex® pomada oftálmica, Alcon S.A., Barcelona, Spain) was applied on the cornea to prevent corneal desiccation. Animals were randomly divided into three groups ($n = 4$ each) and received by intravitreal or subretinal route a sterile suspension of naked plasmid (100 ng) or a sterile suspension based on NOVAFECT O15 polyplexes with a *N*/*P* ratio of 10 or 30 containing 100 ng of the plasmid. Polyplexes and plasmid were resuspended in a total volume of 5 μl of 10 mM HEPES medium, and the pH was adjusted to 7.1 in sterile conditions before injections.

2.9. Subretinal and intravitreal administrations

Under an operating microscope (Zeiss OPMI® pico; Carl Zeiss Meditec GmbH, Jena, Germany) and after piercing the conjunctiva and sclera on the left eye superotemporal region with a 30-gauge needle, a single 4 μl administration of the suspensions was performed with the aid of a 5 μl Hamilton microsyringe (Hamilton Co., Reno, NV) using a bent 34-gauge needle to inject into the vitreous of the left eye, immediately adjacent to the ora serrata without touching the lens, the right advancement of the needle was directly observed. To deliver the suspension into the subretinal space, the needle was passed through the sclerotomy 2 mm posterior to ora serrata and in a tangential direction toward the posterior retinal pole along the subretinal space. Successful administration of suspensions into the subretinal space was confirmed by the appearance of a partial retinal detachment by direct ophthalmoscopy of the eye fundus through the operating microscope. For all the rats, the untreated right eye, which had not been manipulated, served as a normal counterpart or control. Seventy-two hours post-injection, the rats from each experimental group (DNA treated group, and groups treated with NOVAFECT O15 polyplexes at *N*/*P* ratio 10 or 30) were sacrificed by an i.p. injection of an overdose of a 20% sodium pentobarbital solution (Dolethal Vetoquinol®; Especialidades Veterinarias, S.A., Alcobendas, Madrid, Spain) and perfused transcardially with 0.9% saline followed by 4% paraformaldehyde in 0.1 M phosphate-buffered (PBS; pH 7.2–7.4) at 4 °C.

2.10. Evaluation of EGFP expression in rat retinas

For whole-mount preparations, both eyes from two rats of each group were enucleated and immersed for 1 h in a solution of 4%

paraformaldehyde in PBS. Later, the retinas were dissected as wholemounts by making four radial cuts in the superior, inferior, nasal, and temporal retinal poles. Retinal orientation was maintained by making the deepest radial cut in the superior retina. The retinas were postfixed for 1 h in the same fixative, rinsed in PBS, and mounted vitreal side up on poly-L-lysine coated microscope slides, covered with anti-fading mounting media containing 50% glycerol and 0.04% *p*-phenylenediamine in 0.1 M sodium carbonate buffer (pH 9.0).

For sagital section preparations, both eyes from two rats of each group were enucleated, and the anterior segments, including the lens, were removed. Posterior eyecups were fixed for 1 h with 4% paraformaldehyde in 0.1 M PBS, followed by several washes in PBS. Samples were then immersed in 30% sucrose in PBS overnight at 4 °C for cryoprotection. Eyecups were embedded and oriented in optimal cutting temperature (O.C.T.™) compound (Tissue-Tek®; Sakura Finetek Europe B.V., Alphen and den Rijn, The Netherlands) and frozen in 2-methylbutane cooled in liquid nitrogen at −60 °C. Radial sections (15 μm) were cut with a cryostat (HM 550; Microm International GmbH, Walldorf, Germany), mounted on SuperFrost® Plus microscope slides (VWR International bvba, Leuven, Belgium). To counterstain, all retinal nuclei sections were stained with 5 μg/ml Hoechst 33342 dye (Sigma Aldrich) for 5 min and then thoroughly washed with PBS 0.1 M and covered with anti-fading mounting media. GFP expression and DAPI staining were evaluated by spectral confocal microscopy (Leica TCS SPE).

2.11. Statistical analysis

Statistical analysis was performed using the InStat program (GraphPad Software, San Diego, CA, USA). Differences between groups at significance levels of 95% were calculated by the student's *t* test. In all cases, *P* values <0.05 were considered as statistically significant. Normal distribution of samples was assessed by the Kolmogorov–Smirnov test and the homogeneity of the variance by the Levene test. Data were presented as mean ± SD, unless stated otherwise.

3. Results

3.1. Cryo-TEM

Cryo-TEM is frequently used for the visual characterization of biocomplexes such as chitosan/DNA polyplexes. Fig. 1 shows a heterogeneous population polyplexes with most of them having a particle size less than 200 nm, in agreement with the DLS characterization shown in Fig. 2.

3.2. Measurements of size and zeta potential

The average size and zeta potential of polyplexes are shown in Fig. 2. Size clearly decreased as the *N*/*P* ratio increased (from 256.5 ± 56 nm at *N*/*P* 10 to 67.3 ± 0.44 nm at *N*/*P* 60), indicating that size of polyplexes is strongly affected by the charge ratio. In contrast, the zeta potential was not substantially affected by the *N*/*P* ratio. Zeta potential values oscillated from 6.3 mV at *N*/*P* 10 to 10.5 mV at *N*/*P* 60. The most evident change observed in zeta potential value was observed when *N*/*P* ratio raised from 10 to 20. In all cases, polydispersity index was below 0.3 (data not shown).

3.3. Gel retardation assays

Fig. 3 shows the results obtained in the agarose electrophoresis gel at different *N*/*P* ratios to study the binding efficiency and protection capacity against DNase I enzymatic digestion of oligochitosans. Lanes 1, 2, and 3 correspond to free DNA (untreated DNA, DNA treated with SDS 1% and DNA incubated with DNase I and treated with SDS 1%, respectively). On lanes 4, 7, 10 and 13, polyplexes were formulated at 5, 10, 20 and 30 *N*/*P* ratios, respectively. Lanes 5, 8, 11 and 14 represent the bands of those *N*/*P* ratios treated with SDS 1% to release the DNA from oligochitosans, and in lanes 6, 9, 12 and 15, polyplexes were incubated with DNase I and then treated with SDS 1%. The absence of signal in lane 3 suggests that the enzyme worked properly. From Fig. 3 can be observed that our formulations were able to complex, release and protect the plasmid, depending on the *N*/*P* ratio.

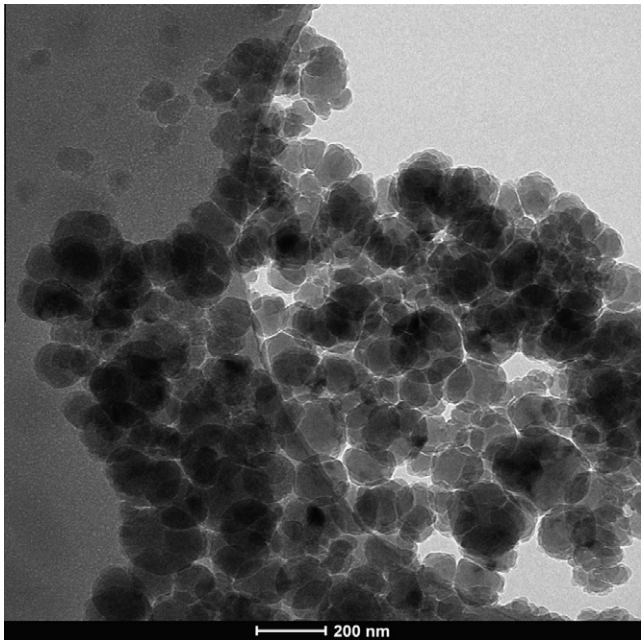

Fig. 1. Cryo-TEM micrograph of oligochitosan/DNA polyplexes at *N*/*P* 20, suspended on HEPES medium 10 mM, pH 7.1.

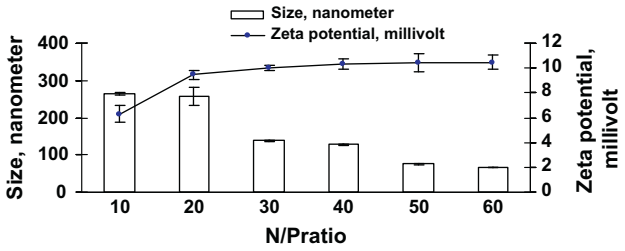

Fig. 2. Effect of *N*/*P* ratio on size and zeta potential of oligochitosan/DNA polyplexes suspended in HEPES medium 10 mM, pH 7.1 (mean ± SD, *n* = 3). (For interpretation of the references to color in this figure legend, the reader is referred to the web version of this article.)

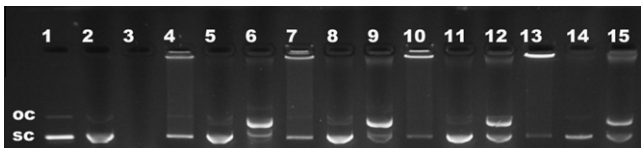

Fig. 3. Binding efficiency between oligochitosans and DNA at different *N*/*P* ratios and protection capacity from DNase I enzymatic digestion visualized by agarose gel electrophoresis. OC: open circular form, SC: supercoloid form. Lanes 1–3 correspond to free DNA; lanes 4–6, *N*/*P* = 5; lanes 7–9, *N*/*P* = 10; lanes 10–12, *N*/*P* = 20; lanes 13–15, *N*/*P* = 30. Polyplexes were treated with SDS (lanes 2, 5, 8, 11, and 14) and DNase I (lanes 3, 6, 9, and 15).

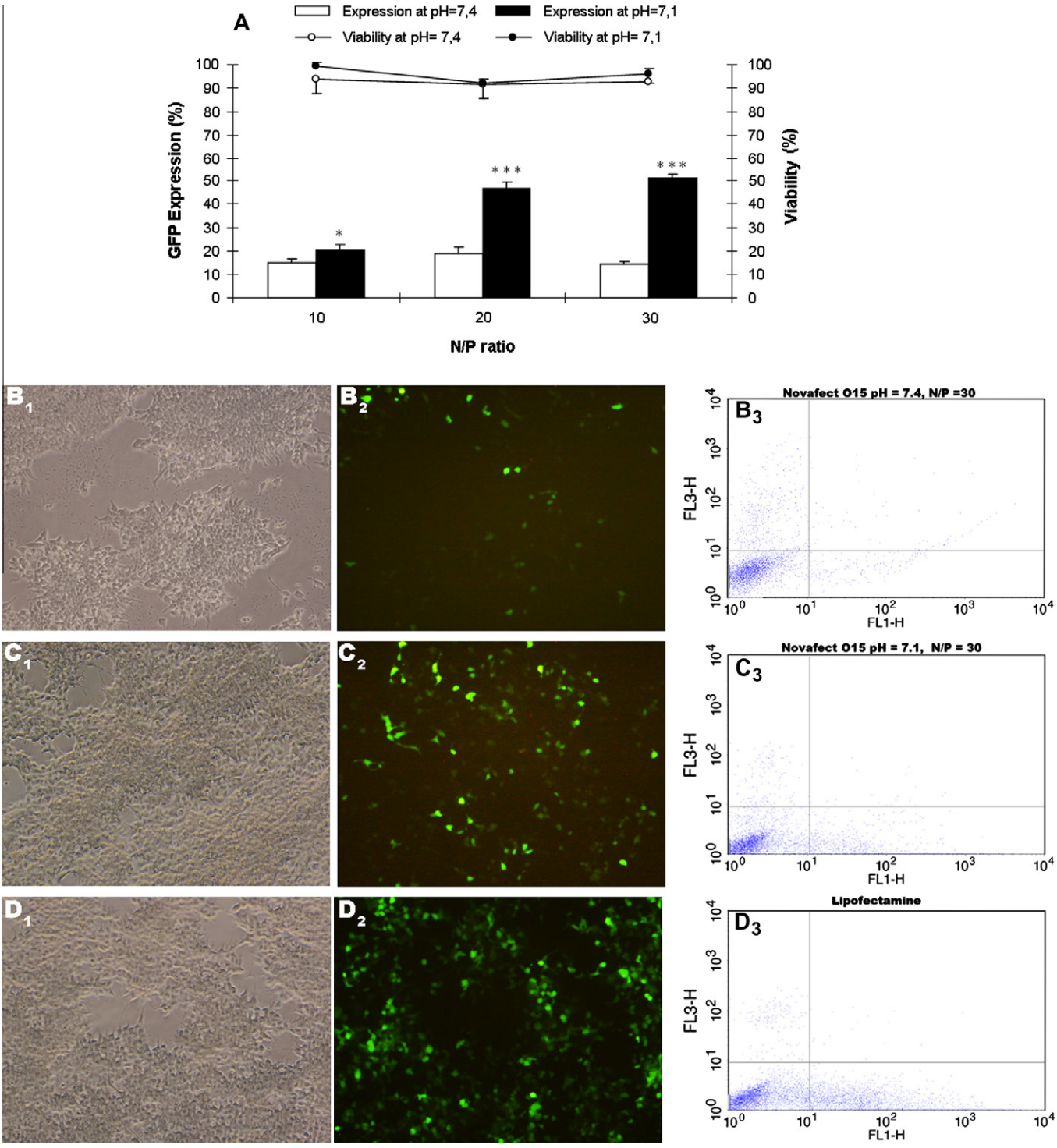

Fig. 4. Transfection efficiency of oligochitosan/DNA polyplexes in HEK-293 cells. (A) Influence of *N*/*P* ratio and pH on EGFP expression and viability in HEK-293 cells. Transfection data were normalized to Lipofectamine™ 2000 (mean ± SD; $n = 3$). At all *N*/*P* ratio tested, statistical differences were reached when compared the GFP expression at pH 7.4 and 7.1. $^{*}p < 0.05$ at *N*/*P* 10, and $^{***}p < 0.001$ at *N*/*P* 20 and 30. (B_1) Contrast phase image, (B_2) fluorescent image, and (B_3) flow cytometry dot-plot (FL_1/FL_3) of HEK-293 cells transfected with polyplexes at pH 7.4 and a *N*/*P* ratio of 30. (C_1) Contrast phase image, (C_2) fluorescent image, and (C_3) flow cytometry dot-plot (FL_1/FL_3) of HEK-293 cells transfected with polyplexes at pH 7.1 and a *N*/*P* ratio of 30. (D_1) Contrast phase image, (D_2) fluorescent image, and (D_3) flow cytometry dot-plot (FL_1/FL_3) of HEK-293 cells transfected with Lipofectamine™ 2000. Images were acquired at 3 days post-transfection, original magnification 20×.

3.4. Transfection efficiency in HEK-293 cells

Prior to the evaluation of the polyplexes in animal studies, we studied the influence of the pH on the transfection efficiency in HEK-293 cells. As observed in Fig. 4A (bars), transfection levels in HEK-293 cells depended on both the *N*/*P* ratio and the pH of the transfection medium (data normalized to Lipofectamine™ 2000). At each one of the *N*/*P* ratio tested, transfection efficiency was significantly higher at pH 7.1 than at pH 7.4 ($^{*}p < 0.05$ at *N*/*P* 10, $^{***}p < 0.001$ at *N*/*P* 20 and 30). Maximum EGFP expression was

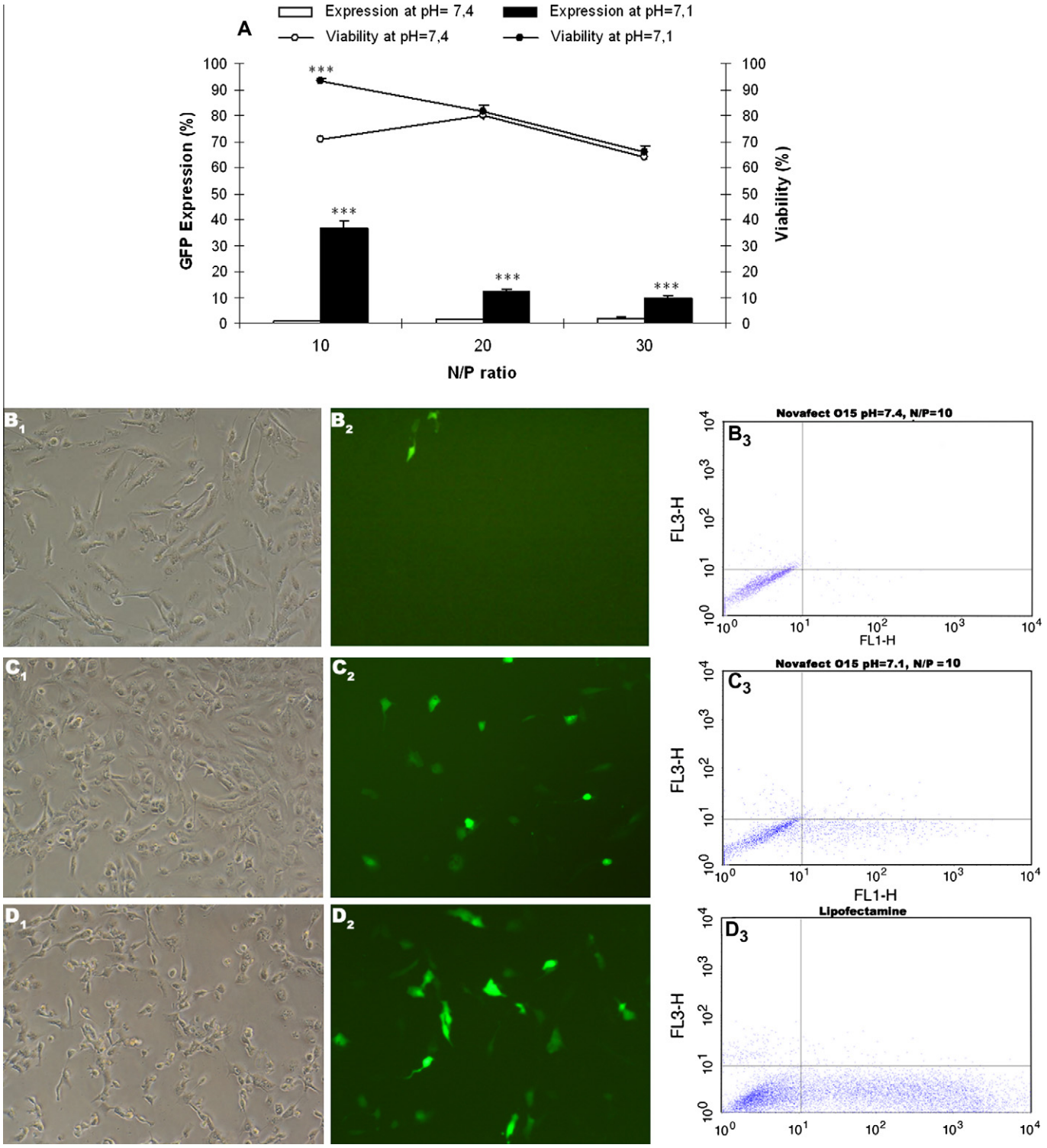

Fig. 5. Transfection efficiency of oligochitosan/DNA polyplexes in ARPE-19 cells. (A) Influence of *N*/*P* ratio and pH on GFP expression and viability in ARPE-19 cells. Transfection data were normalized to Lipofectamine™ 2000 (mean ± SD; $n = 3$). At all *N*/*P* ratio tested, statistical differences were reached when compared the GFP expression at pH 7.4 and 7.1 $^{***}p < 0.001$. (B_1) Contrast phase image, (B_2) fluorescent image, and (B_3) flow cytometry dot-plot (FL_1/FL_3) of ARPE-19 cells transfected with polyplexes at pH 7.4 and a *N*/*P* ratio of 10. (C_1) Contrast phase image, (C_2) fluorescent image, and (C_3) flow cytometry dot-plot (FL_1/FL_3) of ARPE-19 cells transfected with polyplexes at pH 7.1 and a *N*/*P* ratio of 10. (D_1) Contrast phase image, (D_2) fluorescent image, and (D_3) flow cytometry dot-plot (FL_1/FL_3) of ARPE-19 cells transfected with Lipofectamine™ 2000. Images were acquired at 72 h post-transfection, original magnification 20×.

achieved at *N*/*P* ratio 30, pH 7.1 (51.49%). There was no significant difference in cell viability at the two pH values tested. Fig. 4B and C represents the microscope photographs and flow cytometry dot-plots (FL_1/FL_3) of HEK-293 cells transfected with polyplexes based on NOVAFECT O15 chitosan at a fixed *N*/*P* ratio of 30 and a pH value of 7.4 (Fig. 4B) and 7.1 (Fig. 4C), respectively. Fig. 4D

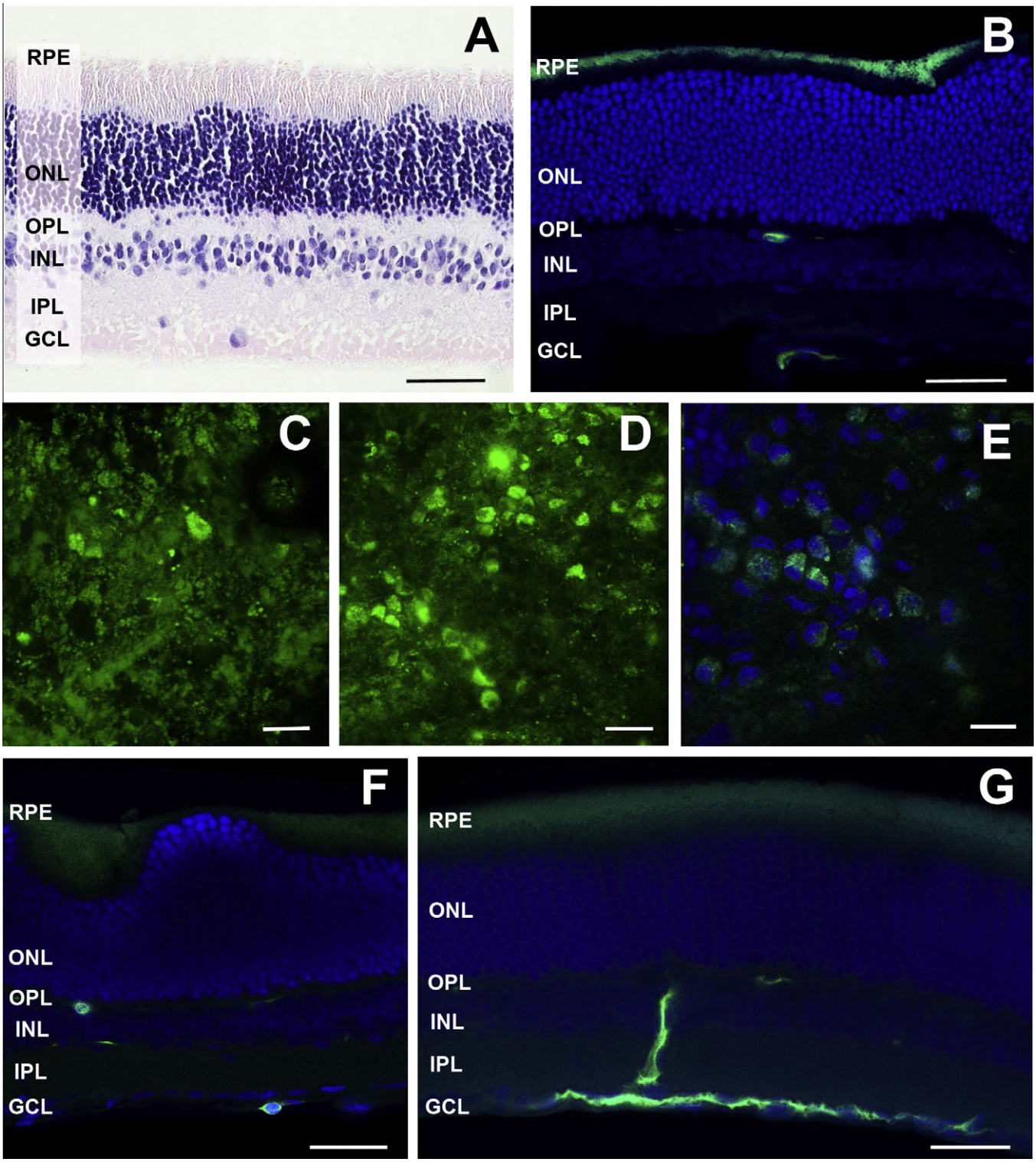

Fig. 6. *In vivo* gene expression of EGFP after subretinal administration of oligochitosan/DNA polyplexes at *N*/*P* ratio of 10 to rats. (A) Hematoxylin–eosin rat retina cross-section, showing the different layers of the retina. RPE (Retinal Pigment Epithelium layer), ONL (Outer nuclear layer), OPL (Outer plexiform layer), INL (Inner nuclear layer), IPL (Inner plexiform layer), GCL (Ganglion cell layer). (B) Fluorescent microscopy image of a 5-μm treated retina cross-section. EGFP expression with Hoechst 33342 staining of cell nuclei. (C–E) Whole-mount views of several retinas focused at the RPE. (F) Vertical section showing transfection in some horizontal and ganglion cells. (G) High EGFP expression in Müller cells. Scale bar = 50 μm.

corresponds to Lipofectamine™ 2000. A statistically significant enhancement in transfection efficiency, without affecting cell viability, was achieved when the pH of the transfection medium changed from 7.4 to 7.1.

3.5. Transfection efficiency and cell viability in ARPE-19 cells

As observed in Fig. 5A (bars), transfection in ARPE-19 cells was practically non-existent at pH 7.4; however, transfection efficiency

drastically increased to 36.5% (data normalized to Lipofectamine™ 2000) when pH of the transfection medium changed from 7.4 to 7.1 at a *N*/*P* ratio of 10 ($^{***}p < 0.001$). In contrast to HEK-293 cells, viability decreased as the *N*/*P* ratio increased. At *N*/*P* 10, cell viability at pH 7.1 (93.19%) was higher than at pH 7.4 (70.8%), $^{***}p < 0.001$. No significant differences were observed in viability at *N*/*P* ratios of 20 and 30. Fig. 5B and C represents the microscope photographs and flow cytometry dot-plots (FL_1/FL_3) of ARPE-19 cells transfected with polyplexes based on NOVAFECT O15 oligochitosans at a fixed *N*/*P* ratio of 10 and a pH value of 7.4 (Fig. 5B) and 7.1 (Fig. 5C), respectively. Fig. 5D corresponds to Lipofectamine™ 2000. A statistically significant enhancement in transfection efficiency was achieved when the pH of the transfection medium changed from 7.4 to 7.1 ($^{***}p < 0.001$).

3.6. EGFP expression after subretinal injection of oligochitosan/DNA polyplexes

Two formulations of polyplexes at *N*/*P* 10 and 30, and one naked plasmid DNA suspension as control, were administered by the subretinal route in order to evaluate the transfection efficiency in different layers of the rat retina. 72 h post-injection, significant EGFP expression was detected only in the group treated with oligochitosan/DNA polyplexes at *N*/*P* 10 (Fig. 6). No gene expression was observed after the administration of naked plasmid DNA, and little-to-no transfection was detected with polyplexes at *N*/*P* 30 (data not shown).

High levels of EGFP expression were found mainly in the RPE layer. Fig. 6 shows EGFP expression in the RPE in vertical sections (Fig. 6B) as well as in whole-mount processed retinas (Fig. 6C–E). A modest expression was found in the remaining layers of the retina, particularly in the outer plexiform layer (Fig. 6B and F) and in the ganglion cells layer (Fig. 6F and G). As show in Fig. 6G, high levels of EGFP expression were also found in some Müller cells after subretinal injections at *N*/*P* 10.

3.7. EGFP expression after intravitreal injection of oligochitosan/DNA polyplexes

Following the same protocol as performed for subretinal administrations, two formulations of polyplexes at *N*/*P* 10 and 30 and one naked plasmid DNA suspension were injected intravitreally to evaluate the transfection efficiency in different layers of the rat retina. 72 h post-injection, only significant EGFP expression was detected in the group treated with *N*/*P* 10 ratio.

After intravitreal injection, the EGFP expression was found mainly in the retinal ganglion cells as observed in Fig. 7. We also found some positive expression at the outer nuclear layer, suggesting positive expression of horizontal cells and/or Müller cell processes. When Hoechst 33342 was used to label cell nuclei, we observed an important percentage of ganglion cells transfected on a wide surface of the injected retinas (Fig. 7C). Very little expression was detected in the RPE.

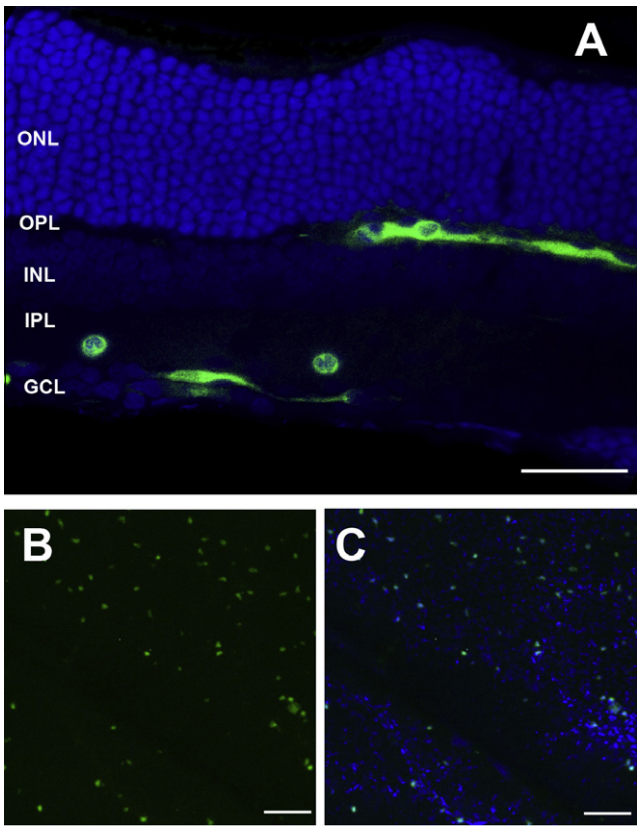

Fig. 7. *In vivo* gene expression of EGFP after intravitreal administration of oligochitosan/DNA polyplexes at a *N*/*P* ratio of 10 to rats. (A) Fluorescent microscopy image of a 5-μm treated retina cross-section. EGFP expression is localized mainly at the retinal ganglion cells. Sometimes, as in this example, high EGFP expression can be observed at the OPL. Scale bar = 50 μm. (B) EGFP expression and (C) colocalization of GFP expression with Hoechst 33342 staining of cell nuclei in a treated retina, whole-mounted vitreous side up. An extensive expression can be observed in many retinal ganglion cells through the whole retina. Scale bar = 100 μm.

4. Discussion

The present study was designed to investigate the potential use of polyplexes based on oligochitosans for retinal gene therapy purposes. A selected formulation with a *N*/*P* ratio of 10 led to significant EGFP expression in different layers and cells of the retina when administered to rats by both subretinal and intravitreal injections.

We prepared polyplexes based on NOVAFECT O15 oligochitosans by the self-assembly method and visualized them by Cryo-TEM (Fig. 1). DNA compaction with chitosan may exhibit different structures depending basically on the characteristics of the plasmid, the chitosan, the *N*/*P* ratio, and the solution properties like ionic strength and pH [30,31]. In our hands, a selected formulation based on *N*/*P* = 20 suspended in HEPES medium 10 mM at pH 7.1 was seen as a heterogeneous population of polyplexes. Most of the polyplexes had a particle size inferior to 200 nm, which is in agreement with particle size studies at different *N*/*P* ratios (Fig. 2). For all formulations studied, the zeta potential value was positive, due to the presence of residual protonated amino groups of chitosan that did not take part in the neutralization with negatively charged DNA, although clearly inferior to that reported by other authors [18,28] with the same NOVAFECT O15 oligochitosans. Such differences may be explained in part, by the fact that the zeta potential value strongly depends on the pH and on the ionic strength of the measurement medium [15]. In addition, the approximation model employed to calculate the zeta potential is another important factor to be considered [32]. Our data revealed an increase in the value of the zeta potential as the charge ratio increased, especially when the *N*/*P* ratio increased from 10 to 20. At this point, the zeta potential appears to reach a maximum value as observed in previous studies [16,33]. Regarding particle size, many factors have been found that influence on the size of polyplexes based on chitosans, such as MW and DDA of the chitosan, the pH and the ionic strength of the measurement medium, the preparation method, or the characteristic of the plasmid accomplished

[15,16,30,34]. Particle sizes were indirectly proportional to the charge ratio, with values oscillating from 256.5 ± 56 nm at *N*/*P* 10 to 67.3 ± 0.44 nm at *N*/*P* 60. Based on these observations, we suggest that an increase in the amount of oligochitosan results in a more efficient condensation of the plasmid, which finally generates more positively charged polyplexes and smaller particles sizes.

As expected from the agarose gel electrophoresis assays, DNA condensation, protection, and release from the polyplexes depended on the *N*/*P* charge (Fig. 3). From lanes 4, 7, 10 and 13, we observe that the binding efficiency increased proportionally with the charge ratios as stated by the intensity of the white band. At all charge ratios studied, SDS 1% treatment (lanes 5, 8, 11 and 14) was able to release the plasmid from the oligochitosan; however, the lower intensity of the white band at 30 charge ratio (lane 14) suggests that at this point, the plasmid was more efficiently complexed with the chitosan and therefore was more difficult to be released, probably due to the fact that polyplexes were more positively charged. Interestingly, all ratios protected the plasmid from enzymatic digestion (lanes 6, 9, 12, and 15), although the most intensive signal of the supercoloid form (SC), the most bioactive form ([35,36], was detected at lane 12 (*N*/*P* 20). Lanes 6 and 9 had intensive signals on the open circular form (OC), which indicates enzymatic digestion. The polyplexes loaded in lane 15 (*N*/*P* 30), protected against enzymatic digestion, however most of the plasmid was retained in the well; therefore, we did not check charge ratios over 30, since an optimum balance between DNA complexation and release is required to increase transfection efficiency [37].

Once we studied that our formulations were biotechnologically suitable for gene therapy purposes, we evaluated *in vitro* the transfection efficiency and cell viability at 72 h in HEK-293 and ARPE-19 cells at pH 7.4 and pH 7.1, because this pH value is similar to that found in the vitreous humor of the rat [29] and has been widely reported that chitosan-mediated transfection efficiency strongly depends on slight changes in the pH value of the transfection medium [11,12,15]. Previously, it has been reported that EGFP expression is maximum at 72 h in these two cell lines [38].

Transfection efficiency in HEK-293 cells drastically increased at all *N*/*P* ratios when pH slightly decreased from 7.4 to 7.1 (Fig. 4). Such an increase in transfection efficiency has been widely attributed to the highly protonated amino groups in the chitosan at low pH [11,12,15], which enhances the binding to the negatively charged plasmid, and therefore, smaller and more stable polyplexes are obtained [39].

In HEK-293 cells, we observed that at pH 7.1, transfection efficiency was correlated with the *N*/*P* charge ratio. Maximum transfection efficiency was reached at *N*/*P* 30. However, in ARPE-19 cells, transfection efficiency at pH 7.1 decreased as the charge ratio increased (Fig. 5). In this case, the highest transfection efficiency was obtained at *N*/*P* 10. These results suggest that chitosan-mediated transfection efficiency depends on the cell type, and therefore, it is necessary to test different conditions for each cell line [40,41].

Once oligochitosan polyplexes were able to transfect *in vitro* ARPE-19 cells at pH 7.1, we administered these polyplexes to Sprague–Dawley rats by subretinal and intravitreal injections. Based on the assumption that each cell line requires different conditions to be efficiently transfected [40,41] and that polyplexes uptake and intracellular trafficking may differ between *in vitro* and *in vivo* conditions [42], we administered polyplexes at two *N*/*P* ratios, 10 and 30, in order to evaluate the transfection efficiency in different layers of the rat retina. Best EGFP expression were obtained when polyplexes where administered at *N*/*P* ratio 10 by both subretinal and intravitreal injections. Little-to-no transfection was detected with the polyplexes at *N*/*P* 30, and no gene expression at all was observed after naked plasmid DNA administration (data not shown), as reported by other authors [43,44].

We selected the intravitreal and subretinal administration routes because both are clinically viable delivery options and are considered the two most effective ways to deliver material to the back of the eye [42]. In addition, each route can target different cells of the retina [24,45,46].

Subretinal injections of our polyplexes at *N*/*P* 10 substantially transfected RPE cells and some photoreceptors in the proximity of the injection site, but no significant expression was detected in other areas of the retina distal to the injection site (Fig. 6). However, we observed some expression of our reported gene in some cells of the inner nuclear and plexiform layers (Fig. 6) close to the injection site, suggesting that subretinal administration has a localized effect and can partially diffuse from the subretinal space of the injection site to the inner layers of the retina. Therefore, subretinal injections demonstrated a significant utility to transfect RPE cells, which is a very interesting target tissue for gene delivery, as it may serve as a platform for secretion of transgene products to the neuronal retina or chorioretinal vasculature and plays a major role in ocular diseases associated with senescence and dystrophies of the photoreceptors [25,47].

Intravitreally injected polyplexes at *N*/*P* 10 expressed our reported gene mainly in the retinal ganglion cell layer and in some cells of the inner nuclear and plexiform layers of the retina. Upon examination of fluorescence from retinal sections vitreous side up mounted, intravitreally injected polyplexes produced a more uniform distribution of the EGFP expression through the whole surface of the retina, as can be observed in Fig. 7. Therefore, vitreous humor does not represent a barrier that hampers the diffusion of our polyplexes through electrostatic interactions between the positively charged polyplexes and the negatively charged glycosaminoglycans (GAGs) of the vitreous, which would generate aggregates that hamper the transport of the polyplexes [48]. The significant expression of our reported gene found in the inner nuclear and plexiform layers of the retina suggest that this mode of therapy could be applicable to treat some pathologies of the retina such us X linked juvenile retinoschisis disease [24].

Taken together, our *in vivo* data suggest that polyplexes based on low molecular weight ultrapure oligochitosans can transfect different non-dividing cells of the retina depending on the administration route. We did not find evidence of inflammation in the histological sections of the retina, which suggest that this methodology does not have any overtly damaging consequences to retinal cells.

5. Conclusion

We elaborated and characterized polyplexes based on low molecular weight and highly deacetylated ultrapure oligochitosans and studied their capacity to deliver nucleic acids in the rat retina. Resulted polyplexes were biotechnologically suitable for gene therapy purposes, as they were able to retain, protect, and release the plasmid. In addition, polyplexes were positively charged and size oscillated in the nanometric range, depending on the *N*/*P* ratio. *In vitro* studies revealed a drastic increase in the transfection efficiency when the pH of the transfection medium changed from 7.4 to 7.1 in both HEK-293 and ARPE-19 cells.

Subretinal injections transfected cells mainly in the RPE layer, whereas intravitreal injections transfected cells mainly in the ganglion cell layer and in the inner nuclear and plexiform layers of the retina. This treatment strategy appears to be a safely and clinically viable novel approach to deliver DNA to retinal cells; however, additional studies may be required to explore the properties of this promising material as gene carrier for retinal therapy purposes. Classically, oligochitosans have been considered as a building block for the design of more sophisticated biomaterials;

therefore, smart chemical modifications of the main block with appropriate ligands could result in more specific and more efficient materials.

Acknowledgments

This project was partially supported by the University of the Basque Country UPV/EHU (UFI 11/32), by the Research Chair in Retinitis Pigmentosa "Bidons Egara", and by the National Organization of Spanish Blind People (ONCE). Technical and human support provided by SGIker (UPV/EHU) is gratefully acknowledged.

References

[1] S.F. Alino, M. Bobadilla, J. Crespo, M. Lejarreta, Human alpha 1-antitrypsin gene transfer to *in vivo* mouse hepatocytes, Hum. Gene Ther. 7 (1996) 531–536.
[2] A. Rolland, Gene medicines: the end of the beginning?, Adv Drug Deliv. Rev. 57 (2005) 669–673.
[3] A.E. Smith, Viral vectors in gene therapy, Annu. Rev. Microbiol. 49 (1995) 807–838.
[4] I.M. Verma, N. Somia, Gene therapy – promises, problems and prospects, Nature 389 (1997) 239–242.
[5] M.J. Lim, S.H. Min, J.J. Lee, I.C. Kim, J.T. Kim, D.C. Lee, N.S. Kim, S. Jeong, M.N. Kim, K.D. Kim, J.S. Lim, S.B. Han, H.M. Kim, D.S. Heo, Y.I. Yeom, Targeted therapy of DNA tumor virus-associated cancers using virus-activated transcription factors, Mol. Ther. 13 (2006) 899–909.
[6] R.I. Mahato, A. Rolland, E. Tomlinson, Cationic lipid-based gene delivery systems: pharmaceutical perspectives, Pharm. Res. 14 (1997) 853–859.
[7] M. Lee, J.W. Nah, Y. Kwon, J.J. Koh, K.S. Ko, S.W. Kim, Water-soluble and low molecular weight chitosan-based plasmid DNA delivery, Pharm. Res. 18 (2001) 427–431.
[8] S.C. Richardson, H.V. Kolbe, R. Duncan, Potential of low molecular mass chitosan as a DNA delivery system: biocompatibility, body distribution and ability to complex and protect DNA, Int. J. Pharm. 178 (1999) 231–243.
[9] S. Mansouri, P. Lavigne, K. Corsi, M. Benderdour, E. Beaumont, J.C. Fernandes, Chitosan–DNA nanoparticles as non-viral vectors in gene therapy: strategies to improve transfection efficacy, Eur. J. Pharm. Biopharm. 57 (2004) 1–8.
[10] F.C. MacLaughlin, R.J. Mumper, J. Wang, J.M. Tagliaferri, I. Gill, M. Hinchcliffe, A.P. Rolland, Chitosan and depolymerized chitosan oligomers as condensing carriers for *in vivo* plasmid delivery, J. Control. Release 56 (1998) 259–272.
[11] T. Sato, T. Ishii, Y. Okahata, *In vitro* gene delivery mediated by chitosan. effect of pH, serum, and molecular mass of chitosan on the transfection efficiency, Biomaterials 22 (2001) 2075–2080.
[12] T. Ishii, Y. Okahata, T. Sato, Mechanism of cell transfection with plasmid/chitosan complexes, Biochim. Biophys. Acta 1514 (2001) 51–64.
[13] S. Mao, W. Sun, T. Kissel, Chitosan-based formulations for delivery of DNA and siRNA, Adv. Drug Deliv. Rev. 62 (2010) 12–27.
[14] M. Lavertu, S. Methot, N. Tran-Khanh, M.D. Buschmann, High efficiency gene transfer using chitosan/DNA nanoparticles with specific combinations of molecular weight and degree of deacetylation, Biomaterials 27 (2006) 4815–4824.
[15] S. Nimesh, M.M. Thibault, M. Lavertu, M.D. Buschmann, Enhanced gene delivery mediated by low molecular weight chitosan/DNA complexes: effect of pH and serum, Mol. Biotechnol. 46 (2010) 182–196.
[16] H.Q. Mao, K. Roy, V.L. Troung-Le, K.A. Janes, K.Y. Lin, Y. Wang, J.T. August, K.W. Leong, Chitosan–DNA nanoparticles as gene carriers: synthesis, characterization and transfection efficiency, J. Control. Release 70 (2001) 399–421.
[17] S.P. Strand, S. Danielsen, B.E. Christensen, K.M. Varum, Influence of chitosan structure on the formation and stability of DNA-chitosan polyelectrolyte complexes, Biomacromolecules 6 (2005) 3357–3366.
[18] E.A. Klausner, Z. Zhang, R.L. Chapman, R.F. Multack, M.V. Volin, Ultrapure chitosan oligomers as carriers for corneal gene transfer, Biomaterials 31 (2010) 1814–1820.
[19] M. Koping-Hoggard, I. Tubulekas, H. Guan, K. Edwards, M. Nilsson, K.M. Varum, P. Artursson, Chitosan as a nonviral gene delivery system. Structure–property relationships and characteristics compared with polyethylenimine *in vitro* and after lung administration *in vivo*, Gene Ther. 8 (2001) 1108–1121.
[20] M. Koping-Hoggard, Y.S. Mel'nikova, K.M. Varum, B. Lindman, P. Artursson, Relationship between the physical shape and the efficiency of oligomeric chitosan as a gene delivery system *in vitro* and *in vivo*, J. Gene Med. 5 (2003) 130–141.
[21] C. Andrieu-Soler, R.A. Bejjani, T. de Bizemont, N. Normand, D. BenEzra, F. Behar-Cohen, Ocular gene therapy: a review of nonviral strategies, Mol. Vis. 12 (2006) 1334–1347.
[22] L.N. Johnson, S.M. Cashman, R. Kumar-Singh, Cell-penetrating peptide for enhanced delivery of nucleic acids and drugs to ocular tissues including retina and cornea, Mol. Ther. 16 (2008) 107–114.
[23] Y. Zhang, F. Schlachetzki, J.Y. Li, R.J. Boado, W.M. Pardridge, Organ-specific gene expression in the rhesus monkey eye following intravenous non-viral gene transfer, Mol. Vis. 9 (2003) 465–472.
[24] D. Delgado, A. Del Pozo-Rodriguez, M.A. Solinis, M. Aviles, B.H. Weber, E. Fernandez, A. Rodriguez Gascon, Dextran and protamine-based solid lipid nanoparticles as potential vectors for the treatment of X linked juvenile retinoschisis, Hum. Gene Ther. 23 (2012) 345–355.
[25] R.A. Bejjani, D. BenEzra, H. Cohen, J. Rieger, C. Andrieu, J.C. Jeanny, G. Gollomb, F.F. Behar-Cohen, Nanoparticles for gene delivery to retinal pigment epithelial cells, Mol. Vis. 11 (2005) 124–132.
[26] M. de la Fuente, B. Seijo, M.J. Alonso, Bioadhesive hyaluronan-chitosan nanoparticles can transport genes across the ocular mucosa and transfect ocular tissue, Gene Ther. 15 (2008) 668–676.
[27] P. Paolicelli, M. de la Fuente, A. Sanchez, B. Seijo, M.J. Alonso, Chitosan nanoparticles for drug delivery to the eye, Expert Opin. Drug Deliv. 6 (2009) 239–253.
[28] E.A. Klausner, Z. Zhang, S.P. Wong, R.L. Chapman, M.V. Volin, R.P. Harbottle, Corneal gene delivery: chitosan oligomer as a carrier of CpG rich, CpG free, or S/MAR plasmid DNA, J. Gene Med. 14 (2011) 100–108.
[29] S. Bassnett, G. Duncan, Direct measurement of pH in the rat lens by ion-sensitive microelectrodes, Exp. Eye Res. 40 (1985) 585–590.
[30] S. Danielsen, K.M. Varum, B.T. Stokke, Structural analysis of chitosan mediated DNA condensation by AFM: influence of chitosan molecular parameters, Biomacromolecules 5 (2004) 928–936.
[31] G. Maurstad, S. Danielsen, B.T. Stokke, The influence of charge density of chitosan in the compaction of the polyanions DNA and xanthan, Biomacromolecules 8 (2007) 1124–1130.
[32] A. Sze, D. Erickson, L. Ren, D. Li, Zeta-potential measurement using the Smoluchowski equation and the slope of the current–time relationship in electroosmotic flow, J. Colloid. Interface Sci. 261 (2003) 402–410.
[33] T. Kiang, J. Wen, H.W. Lim, K.W. Leong, The effect of the degree of chitosan deacetylation on the efficiency of gene transfection, Biomaterials 25 (2004) 5293–5301.
[34] S. Mansouri, Y. Cuie, F. Winnik, Q. Shi, P. Lavigne, M. Benderdour, E. Beaumont, J.C. Fernandes, Characterization of folate–chitosan–DNA nanoparticles for gene therapy, Biomaterials 27 (2006) 2060–2065.
[35] C.R. Middaugh, R.K. Evans, D.L. Montgomery, D.R. Casimiro, Analysis of plasmid DNA from a pharmaceutical perspective, J. Pharm. Sci. 87 (1998) 130–146.
[36] K. Remaut, N.N. Sanders, F. Fayazpour, J. Demeester, S.C. De Smedt, Influence of plasmid DNA topology on the transfection properties of DOTAP/DOPE lipoplexes, J. Control. Release 115 (2006) 335–343.
[37] M. Alatorre-Meda, P. Taboada, F. Hartl, T. Wagner, M. Freis, J.R. Rodriguez, The influence of chitosan valence on the complexation and transfection of DNA: the weaker the DNA–chitosan binding the higher the transfection efficiency, Colloids Surf. B Biointerfaces 82 (2011) 54–62.
[38] A. del Pozo-Rodriguez, D. Delgado, M.A. Solinis, A.R. Gascon, J.L. Pedraz, Solid lipid nanoparticles for retinal gene therapy: transfection and intracellular trafficking in RPE cells, Int. J. Pharm. 360 (2008) 177–183.
[39] M. Koping-Hoggard, K.M. Varum, M. Issa, S. Danielsen, B.E. Christensen, B.T. Stokke, P. Artursson, Improved chitosan-mediated gene delivery based on easily dissociated chitosan polyplexes of highly defined chitosan oligomers, Gene Ther. 11 (2004) 1441–1452.
[40] D. Luo, W.M. Saltzman, Enhancement of transfection by physical concentration of DNA at the cell surface, Nat. Biotechnol. 18 (2000) 893–895.
[41] C.L. Gebhart, A.V. Kabanov, Evaluation of polyplexes as gene transfer agents, J. Control. Release 73 (2001) 401–416.
[42] S.M. Conley, M.I. Naash, Nanoparticles for retinal gene therapy, Prog. Retin. Eye Res. 29 (2010) 376–397.
[43] M. Dezawa, M. Takano, H. Negishi, X. Mo, T. Oshitari, H. Sawada, Gene transfer into retinal ganglion cells by *in vivo* electroporation: a new approach, Micron 33 (2002) 1–6.
[44] X. Cai, S.M. Conley, Z. Nash, S.J. Fliesler, M.J. Cooper, M.I. Naash, Gene delivery to mitotic and postmitotic photoreceptors via compacted DNA nanoparticles results in improved phenotype in a mouse model of retinitis pigmentosa, FASEB J. 24 (2010) 1178–1191.
[45] P. Dureau, L. Legat, M. Neuner-Jehle, S. Bonnel, S. Pecqueur, M. Abitbol, J.L. Dufier, Quantitative analysis of subretinal injections in the rat, Graefes Arch. Clin. Exp. Ophthalmol. 238 (2000) 608–614.
[46] R. Farjo, J. Skaggs, A.B. Quiambao, M.J. Cooper, M.I. Naash, Efficient non-viral ocular gene transfer with compacted DNA nanoparticles, PLoS One 1 (2006) e38.
[47] E. Mannermaa, S. Ronkko, M. Ruponen, M. Reinisalo, A. Urtti, Long-lasting secretion of transgene product from differentiated and filter-grown retinal pigment epithelial cells after nonviral gene transfer, Curr. Eye Res. 30 (2005) 345–353.
[48] S.J. Clark, T.D. Keenan, H.L. Fielder, L.J. Collinson, R.J. Holley, C.L. Merry, T.H. van Kuppevelt, A.J. Day, P.N. Bishop, Mapping the differential distribution of glycosaminoglycans in the adult human retina, choroid, and sclera, Invest Ophthalmol. Vis. Sci. 52 (2011) 6511–6521.